Biointerface Research in Applied Chemistry
Open-Access Journal (ISSN: 2069-5837)

Article
Volume 16, Issue 3, 2026, 77
https://doi.org/10.33263/BRIAC163.077

Hybrid Structures Containing Silver (Gold) Nanoparticles and Amphotericin B: One-Pot and One-Step Preparation, Antifungal Activity

Nadezhda Samoilova [1,*], Maria Krayukhina [1], Inesa Blagodatskikh [1], Oxana Vyshivannaya [2], Nelya Anuchina [3], Dmitry Popov [3]

[1] A. N. Nesmeyanov Institute of Organoelement Compounds, Russian Academy of Sciences, Vavilov 28, Moscow 119334, Russian Federation, larina@ineos.ac.ru;
[2] Faculty of Physics Lomonosov Moscow State University, Leninskie Gory 1-2, Moscow 119991, Russian Federation, edu.ff@org.msu.ru;
[3] A. N. Bakulev National Medical Research Center of Cardiovascular Surgery of the Ministry of Health of the Russian Federation, Roublyevskoe Shosse 135, Moscow 121552, Russian Federation; 205_kabinet@bakulev.ru;
* Correspondence: samoilova@ineos.ac.ru;

Received: 9.02.2026; Accepted: 16.05.2026; Published: 15.06.2026

Abstract: The use of simple approaches to obtaining hybrid structures containing two bioactive components - amphotericin B (AmB) (substance or medicine) and silver (gold) nanoparticles - is an important and urgent task. Three one-pot and one-step methods for preparing AmB/Ag0 were used and analyzed. In the first one, metal nanoparticles formed in an alkaline medium upon heating; in the second, the effect of electromagnetic radiation on silver ions was used; and in the third, the reducing agent NaBH4 was introduced into the system. For all methods, the ratio AmB/Ag^{+} 1:14 (mol) was used, for AmB/Au^{3+} - 1:5. The reaction of silver nanoparticle formation in the presence of both amphotericin samples is almost complete within 20 minutes under the first convection variant of synthesis; the method using microwave radiation resulted in a tenfold reduction of the reaction time. When an external reducing agent ($NaBH_4$) was introduced into the system, the silver nanoparticles' maturation was virtually complete within 30 minutes. The composites were characterized using TEM, UV–Vis and fluorescence spectroscopy, and the DLS method (DLS R_h^{slow} 15-31 nm). The antifungal activity of the preparations against *Candida albicans* was studied. MIC values for most AmB/Ag^0 composites were in the range 0.52-0.82 mg/mL. Additive participation of bioactive components of these systems was revealed, and synergistic participation for the composite based on the AmB medicine (borohydride method) (MIC sample 0.2 mg/mL). AmB/Au^0 composite showed reduced activity. The elaborated approaches to composite preparation, without the use of organic solvents or complex equipment, have potential for the treatment of mixed fungal and bacterial infections.

Keywords: amphotericin B; Ag (Au) nanoparticles; nanocomposite preparations; antifungal activity.

1. Introduction

Infectious diseases, and in particular fungal infections, are extremely common in the human population. Amphotericin B (AmB) is an important member of the macrolide polyene antibiotics and is indicated for the treatment of a wide range of invasive mycoses. AmB binds to sterols (ergosterols) found in the cell membrane of drug-sensitive fungi. Sequestration of

membrane-bound sterols and the formation of transmembrane channels that disrupt physiological ion transport are among the most frequently discussed molecular mechanisms responsible for AmB's antifungal properties at the initial stage [1–3]. When studying the mechanism of action of AmB, the “Janus face” of AmB was also noted: as a prooxidant or as an antioxidant. This redox role is implied in the mechanism of anti-infectious action of AmB – it can act by multiple mechanisms, involving electron transfer, reactive oxygen and nitrogen species formation, and so on. Emerging free radicals can induce lipid peroxidation in the membranes of target cells [4,5]. With increased use and availability of AmB, the number and diversity of fungal species resistant to this agent are likely to increase in the near future. Resistance to amphotericin B can be divided into primary (intrinsic) and acquired resistance. Reports of polyene-resistant yeasts and molds continue to be received [6,7]. In addition, interactions between Candida species and bacteria have been found in mixed infections [8].

One strategy for overcoming the decrease in microorganism resistance to polyenes and enhancing the drug's antibiotic properties is to include an additional active component in its composition. The use of an approach to obtain complexes combining the properties of an antibiotic and metal nanoparticles with antibacterial properties appears quite relevant [9]. Medicines based on such nanoparticles and antibiotics can not only restore the ability of antibiotics to destroy microorganisms, but also reduce their toxicity and the therapeutic dose [5,10,11]. Due to their antibacterial activity, silver (AgNPs) or gold (AuNPs) nanoparticles can be used as additives to antibiotic drugs [12-14]. There is little evidence of pathogen microorganisms’ resistance to AgNPs [15]. It was shown that conjugation of amphotericin B with silver nanoparticles enhances the effects of the drug against primary amoebic meningoencephalitis caused by *Naegleria fowleri* [16].

It is possible to implement two strategic directions for obtaining water-soluble combination drugs of antibiotics and silver (gold) nanoparticles: 1. mixing antibiotic solutions and pre-prepared and stabilized metal nanoparticles, 2. one-pot method – formation of metal nanoparticles in a solution containing antibiotic and metal cations. In the latter variant, the antibiotic acts as a stabilizer for the resulting nanoparticles and can also serve as a reducing agent for metal cations. The most common approach to preparing amphotericin-metal nanoparticle composites is to mix the antibiotic with separately prepared metal nanoparticles [10,16,17]. It is known to obtain a composite of amphotericin-nanosilver in a bacterial supernatant medium. Amphotericin B can be adsorbed on the surface of biogenic silver nanoparticles [18,19]. However, when using this approach, inactive additives will also appear in the composite, so the drug dose should be increased. In our opinion, it is of interest to develop a one-step, one-pot technique for obtaining the AmB/nanometal complex, in which amphotericin acts as a stabilizer for metal nanoparticles formed in a medium containing the antibiotic. Earlier, AuNPs were produced by using sodium borohydride as a reducing agent in the presence of the drug. Gold nanoparticles conjugation with amphotericin B resulted in enhanced bioactivity against Acanthamoeba castellanii [20]. Silver nanoparticles were synthesized using AmB, which acted both as a reducing and stabilizing/capping agent. In this case, the addition of an organic solvent in the reaction medium was used: dry AmB was dissolved in 2-propanol–water [21].

The aim of this work is to test different approaches to obtaining combined AmB/nanometal preparations, in which the antibiotic serves as a stabilizer for silver (gold) nanoparticles formed in its presence. In this work, three variants of the one-pot approach were used. The proposed approaches do not use organic solvents or complex equipment. In the first

variant, the nucleation reaction of metal nanoparticles occurred in an alkaline medium upon heating, in the second variant, the effect of electromagnetic radiation on the system was used, and in the third variant, a reducing agent was introduced into the system. The study used two samples of amphotericin B - amphotericin B substance (AmB-Sub) and amphotericin B medicine (AmB-Med). The advantages and limitations of the methods used to obtain amphotericin/nanometal preparations are discussed. The antimicrobial properties of the obtained conjugates are studied.

2. Materials and Methods

2.1. Materials.

The reagents $NaBH_4$, $HAuCl_4$ (Sigma-Aldrich, Darmstadt, Germany), $AgNO_3$, $KMnO_4$, and NaOH (all of the analytical grade, "Reahim", Moscow, Russia) were used without purification. Amphotericin B substance (AmB-Sub) was from Fluka, and amphotericin B medicine (AmB-Med) was from "Kurgansintez" (Russian Federation). Silver nanoparticles stabilized by a copolymer of maleic acid with ethylene (EM/Ag^0) were obtained by us earlier [22]. Tested microorganism used - yeast-like fungi *Candida albicans* (*C. albicans*) NCPF3255/ATCC 10231 ("BD MicrotrolTM", Becton Dickinson, USA).

2.2. Instrumentation

The pH of solutions was measured using a Fisher Scientific 300 403.1 pH meter (USA). A Hitachi U-5100 spectrophotometer (Japan) was used to obtain UV-visible absorption spectra.

Transmission electron microscopy (TEM) micrographs were taken on a LEO 912 AB microscope (Omega, Karl Zeiss; Germany) operating at an accelerating voltage of 100 kV. To obtain TEM observational data, a drop of the test solution was placed on a formvar-coated copper grid and then evaporated.

The silver or gold content was determined by non-destructive X-ray fluorescence analysis (VRA-30 X-ray fluorescence spectrometer (Karl Zeiss, Jena).

Static and dynamic light scattering (SLS-DLS) studies were carried out on a Photocor Complex spectrometer (Russia) equipped with an automatic goniometer and a PhotoCor-FC2 pseudo-cross-correlation photon counting system used in a logarithmic configuration. A He-Ne laser "Uniphase 1135P" (λ = 633 nm, power 10 mW) was used as a light source. The distribution over relaxation times τ was calculated from the correlation functions using the CONTIN method. For every relaxation maximum found in the spectra of the decay times, the average decay time,, the efficient diffusion coefficient, D, and the hydrodynamic radius, R_h, were calculated using the following relations:

$$ln(\overline{\tau}) = \frac{\sum_i A_i ln(\tau_i)}{\sum_i A_i}, R_h = \frac{k_b T}{6\pi\eta D} = \frac{k_b T}{6\pi\eta} q^2 \overline{\tau}, \quad (1)$$

Where η is the solvent viscosity, k_b is the Boltzmann constant, T is the absolute temperature, and q is the wave vector value. Relative peak width (RPW) was calculated as follows:

$$RPW = \sqrt{\left[\frac{\sum_i (ln(\tau_i))^2 A_i}{\sum_i A_i} - (ln(\overline{\tau}))^2\right]} \quad (2)$$

Measurements of ξ-potential were performed on a Zeta Sizer Nano ZS instrument (Malvern Instruments, Worcestershire, UK).

For microwave synthesis, the system NOVA-2S (Pree Kem, www.sov-lab.ru), 100% power of 800W, and frequency 2450 MHz for 5 s. We used regime -350 W and 70°C.

Fluorescence emission spectra were recorded with a Cary Eclipse Varian spectrofluorometer. The fluorescence spectra were recorded with 1 nm spectral resolution.

2.3. Methods.

2.3.1. Synthesis of AmB/silver (gold) preparations.

2.3.1.1. Method A - heat treatment.

2.3.1.1.1. Synthesis of AmB-Med/Ag^0(T) and AmB-Sub/Ag^0(T).

Freshly prepared solutions of AmB-Med or AmB-Sub in deionized water (20.0 mL, $5.8 \cdot 10^{-5}$ M AmB), $AgNO_3$ (0.16 mL, 0.1 M), and NaOH (0.05 mL, 1 M) were placed in test tubes with screw caps and were intensively mixed. pH of the obtained solution was 10. The reaction mixture was placed in a bath with heated water at 70°C and kept for 20 min. The reaction solution was then stored at room temperature. AmB/Ag^+ molar ratio was 1:14 (mol). For kinetic spectrophotometric measurements, a 0.2 cm cuvette was used; registration was carried out without dilution of the reaction solution. Spectra were recorded at certain time intervals. Dry sample AmB-Med/Ag(T) was obtained after exhaustive dialysis of reaction solution against deionized water (cutoff 1 kDa -1.5 L, 4 changes) with subsequent lyophilic drying (−55°C, 0.05 mbar). The yield of dried AmB-Med/Ag^0 (yellow-brown powder) was 3.6 mg (94.7%). The content of components in the samples was estimated by elemental analysis.

The synthesis of AmB-Sub/Au^0(T) was carried out under the above conditions with the ratio of reagents AmB/Au^{3+} 1:5 (mol). For the reaction, AmB (2.0 mL, $5.8 \cdot 10^{-5}$ M), $HAuCl_4 \cdot 3H_2O$ (0.058 mL, 0.01 M), and NaOH (0.005 mL, 1 M) were mixed.

2.3.1.2. Method B - microwave radiation.

AmB-Sub/Ag^0(M) and AmB-Med/Ag^0(M) were prepared under the above conditions (AmB/Ag^+ molar ratio 1:14 (mol) and pH 10). Reaction solution in the test tube was placed in a microwave oven under the regime 350 W and 70°C. Reactions were carried out by operating in a cycling mode (on 20 s, off 30 s). The reaction observation time was 4 min. The reaction solution was then stored at room temperature. For kinetic spectrophotometric measurements, a 0.2 cm cuvette was used; registration was performed without diluting the reaction solution. Spectra were recorded at certain time intervals.

2.3.1.3. Method C - reduction with $NaBH_4$.

AmB-Sub/Ag^0(B) and AmB-Med/Ag^0(B) were prepared as follows. The freshly prepared solution of $NaBH_4$ (0.032 mL, 0.1 M, 2-fold molar excess with respect to silver ions) was added to the solution of AmB-Med or AmB-Sub (2.0 mL, $5.8 \cdot 10^{-5}$ M AmB, pH 5) with vigorous stirring, and then the $AgNO_3$ (0.016 mL, 0.1 M) was added and shaken vigorously. The molar ratio AmB/$NaBH_4$/Ag^+ was 1:28:14. The reaction mixture was allowed to stand (24 h, 20°C).

2.4. Antifungal test.

For the antifungal test, we used the samples 1 day after preparation. The determination of the minimum inhibitory concentrations (MIC) of the preparations in relation to *C. albicans* was carried out using the method of serial microdilution in accordance with the standard procedure [23].

Initial concentrations of samples were 1.4-1.7 mg/mL. The description of the experiment was given in the protocol published elsewhere [24]. Briefly, all tests were carried out in a 0.2 mL volume using sterile 96-well standard polystyrene plates. The number of wells was dictated by the required dilution range; The last well was left to set up a negative control. For the microorganism under study, the final concentration is 105 CFU/ml. Tryptic soy broth (Bio-Rad Laboratories, USA) in a volume of 0.1 ml was poured into each well of the plate.

Each solution in the volume of 0.1 mL of studied composites in a fourfold ratio to the above-mentioned concentrations was pipetted into the first well containing 0.1 mL of broth. Then 0.1 mL of this mixture was placed to the second well, also initially containing 0.1 mL of broth, and so on. And this procedure was repeated until a sufficient number of dilutions were made. A saline solution with a concentration of 0.45% was used to inoculate a microbial suspension of the test microorganism.

0.1 ml of inoculum was added to the test wells with the appropriate dilution of the test composite, and it was also added to the last well with nutrient broth without the test drug (positive control). The plates with the applied drug, covered with sterile film, were incubated for 48 hours at 35°C. The growth of the culture in the wells in the presence of composites was monitored by comparison with control wells without composites (positive control) under visual control (the wells in the plates were viewed in transmitted light). The MIC of the samples was determined by the lowest concentration of drugs in the well that suppressed the visible growth of the microorganism used.

Statistical processing of data based on the results of 3 measurements was carried out.

3. Results and Discussion

Commercially available products: AmB-Sub (substance) and AmB-Med were used as objects for obtaining and studying AmB composites with metal nanoparticles. AmB-Med – standard parenteral amphotericin product, which contains cholate and deoxycholate to create a stable colloidal dispersion.

Methods of formation and use of composites AmB/Ag^0 (Au^0) are presented in Scheme 1.

First, we carried out one-pot synthesis of colloidal composites of AmB/silver (gold) nanoparticles in an alkaline medium at elevated temperature (T = 70°C, pH = 10) – method A. The reaction proceeds in an alkaline environment, which prevents aggregation of AmB itself and promotes nanoparticle formation [21].

Figure 1 shows the kinetics of formation of amphotericin/metal nanocomposites in an alkaline medium at elevated temperature. The corresponding abbreviations were used for the samples obtained by this method: AmB-Sub/Ag^0 (T), AmB-Med/Ag^0 (T), and AmB-Sub/Au^0 (T).

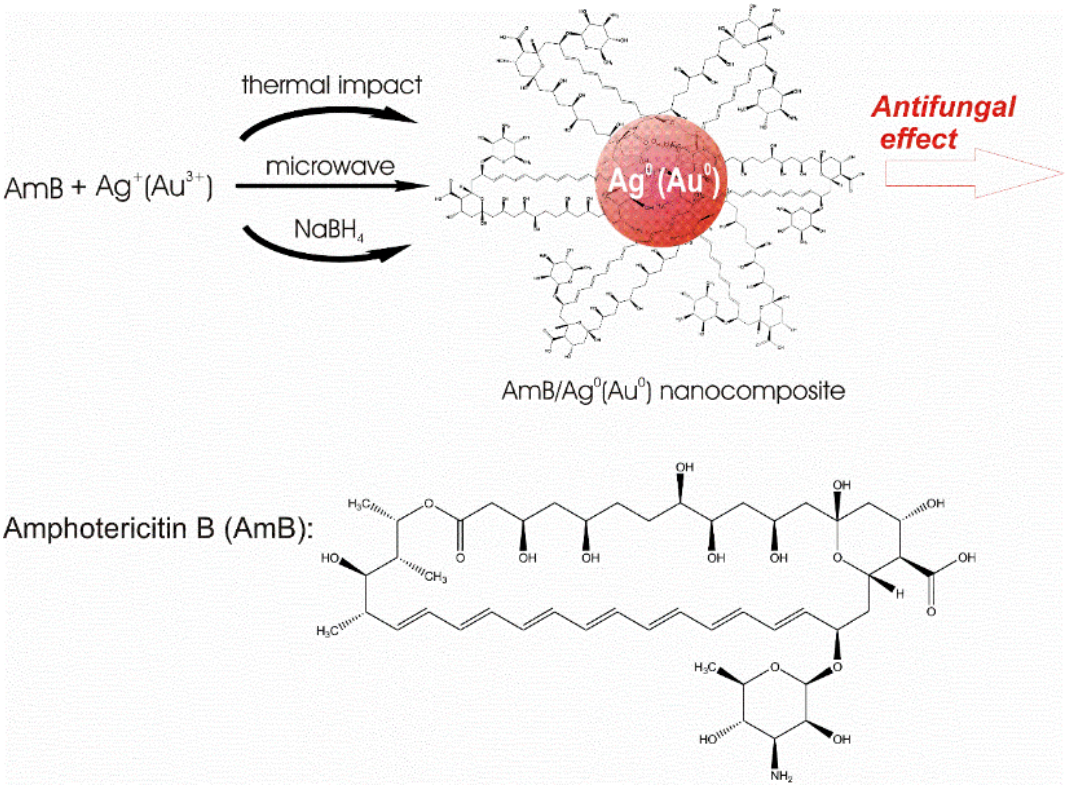

Scheme 1. Production of antifungal composites.

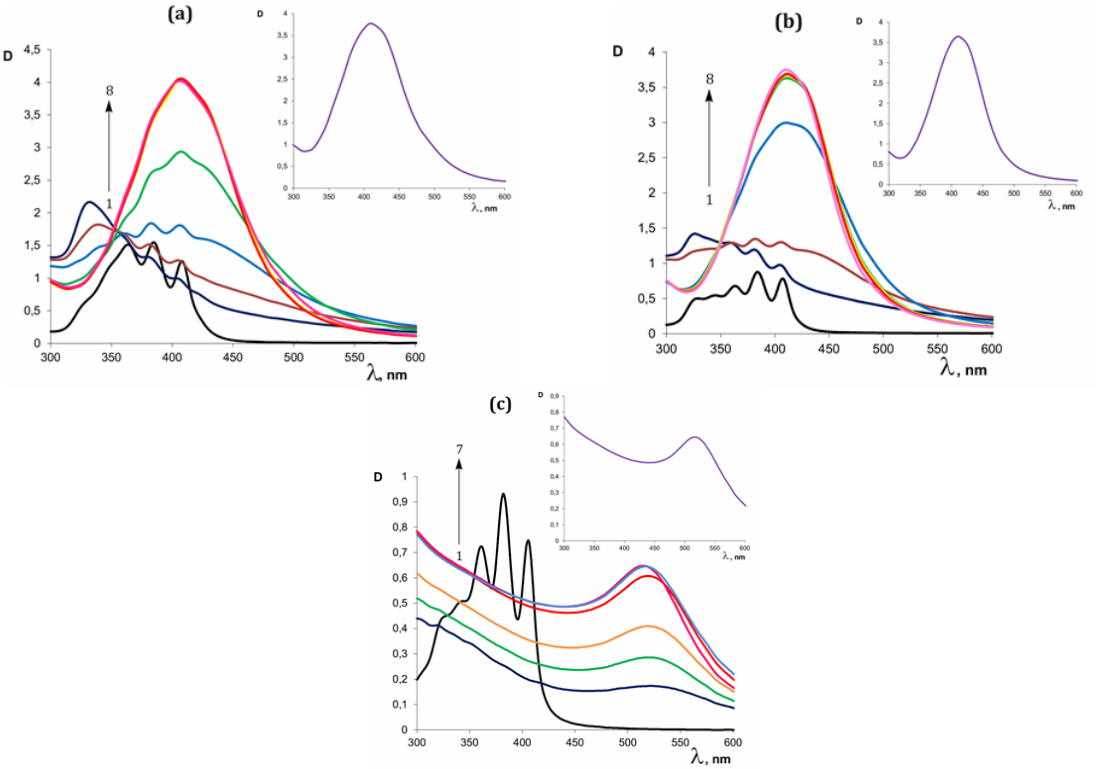

Figure 1. Kinetics of forming the composites: **(a)** AmB-Med/Ag^0 (T); **(b)** AmB-Sub/Ag^0 (T), T=70°C, pH 10, AmB concentration 0.05 mg/mL, the ratio AmB/Ag^+ 1:14 (mol), spectra recording time: 0 (black), 2, 4, 6, 8, 10, 20, 30 min. (from 1 to 8); **(c)** AmB-Sub/Au^0(T), the ratio AmB/Au^{3+} - 1:5 (mol), spectra recording time: 0, 5, 10, 15, 20, 30, 60 min. (from 1 to 7). The insets show spectra after 1-day storage.

As can be seen from Figure 1 (a-c), over time, nanometal particles are formed. In this case, a peak is formed corresponding to the plasmon resonance band. For silver nanoparticles, these values are in the range 410-420 nm, both for the AmB-Med/Ag^o (Figure 1a) and for AmB-Sub/Ag^0 (Figure 1b). The reaction of AgNPs formation in the presence of both

Amphotericin samples is almost complete within 20 minutes. Longer heating (more than 20 minutes) resulted in partial destabilization of the composites. After completion of the reaction and rapid cooling of the reaction mixture to room temperature, the absorption spectrum of the samples remains virtually unchanged - the absorption maximum remains almost at the same level for 24 hours (Figures 1a-c, spectrum at the top right) and even longer (for a month). It should also be noted that AmB-Med/Ag^0 composite samples can be preserved without loss of properties after dialysis (cut-off 1 kDa), lyophilic drying, and stored for at least a year in the refrigerator (UV-Vis and DLS control). AmB-Sub/Ag^0 samples poorly dissolve after drying.

It can also be noted that during the formation of silver nanoparticles in the composite, the characteristic absorption peak at 333 nm, corresponding to the aggregate state of amphotericin, is leveled out [17,21]. During the reaction, monomerization of amphotericin apparently occurs (as evidenced by an absorption band at 405 nm), but this band is obscured by silver nanoparticle absorption. Reducing the pH of the reaction solution to 9 reduced the reaction rate of silver nanoparticle preparation. Thus, for the AmB-Med/Ag^0(T) sample, under these conditions, the reaction is 45% complete in 15 minutes (Figure 2), and at pH 10 – 100% (Figure 1a). pH 12 of the reaction mixture resulted in a polydisperse and less stable product. Increasing the initial AmB/Ag^+ ratio to 1:28 (mol) resulted in a less stable composite; the addition of large amounts of AmB causes it to self-aggregate [17].

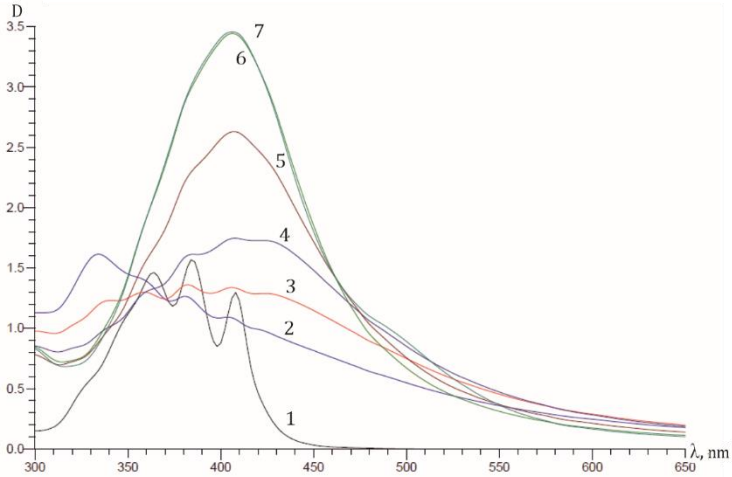

Figure 2. Kinetics of forming of composite AmB-Med/Ag^0 (T), pH 9, t =70°C, AmB concentration 0.05 mg/mL, the ratio AmB/Ag^+ 1/14 (mol/mol). Spectra recording time: 0, 5, 10, 15, 20, 30, 120 min. (from 1 to 7).

For the AmB-Sub/Au^0 sample, the end time of the AuNPs formation reaction is recorded as 30 minutes, while the plasmon resonance band is recorded at 520 nm.

The structure of the amphotericin molecule contains functional groups that have the properties of reducing agents: these are double bonds, secondary hydroxyls (weak reducing agents), and a carbohydrate residue - 3-amino-3,6-dideoxy-D-mannopyranose. It is known that gold cations are stronger oxidizers compared to silver cations (the oxidation-reduction potentials for Ag^+ - Ag^0 and Au^{3+} - Au^0 are + 0.8 and + 1.50 V, respectively). For the most likely oxidation-prone carbohydrate residue in the antibiotic structure, 3-amino-3,6-dideoxy-D-mannopyranose, the electrochemical oxidation potential is not reported in the literature; however, for example, under alkaline conditions, the electrooxidation of D-glucose occurs at +0.8-1.34V.

Previously, it has been shown that there are thermodynamic prerequisites for the spontaneous formation of silver and gold nanoparticles when heated corresponding cations in

an alkaline aquatic environment [25,26]. Oxidation causes structural changes in the antibiotic molecule, and the antifungal activity of the oxidized form of amphotericin (AmB Ox) is significantly reduced in comparison with the native form. The therapeutic index values of AmB Ox were approximately 3-fold lower than those of AmB [27].

To assess the possibility of amphotericin oxidation during the production of complexes with silver (gold) nanoparticles, control experiments were conducted to determine the oxidized form of amphotericin when AmB-Med and AmB-Sub were exposed to potassium permanganate. It was previously noted that when the antibiotic was exposed to oxidizers, changes occurred in the UV-Vis spectrum of amphotericin [28,29]. In this case, there is a decrease in the absorption value at $\lambda = 408$ nm relative to $\lambda = 390$ nm. In our control experiment for AmB-Sub, the ratio of optical densities $D_{\lambda 390}$ /$D_{\lambda 408}$ nm in the initial compound was 1.33, and after oxidation (AmB-Sub Ox), 2.04 (Figure 3A); for AmB-Med, 2.04 and 2.28 (AmB-Med Ox), respectively (Figure 3B). AmB-Sub Ox and AmB-Med Ox are oxidized with $KMnO_4$, and these forms of amphotericin were prepared according to the publication [29]. The same trend was noted in the case of the gold-containing composite AmB-Sub/Au^0 (Figure 3C): the ratio of optical densities $D_{\lambda 390}/D_{\lambda 408}$ nm in the initial compound was 1.37, and after oxidation, 1.6 (AmB-Sub/Au^0), which may indicate oxidation of AmB during the production of this composite. This may occur through the participation of the carbohydrate residue of amphotericin, taking into account the electrode potentials of the carbohydrate and the metal. The thermodynamic prerequisites for the spontaneous reduction of gold cations should also be taken into account under the conditions used [25].

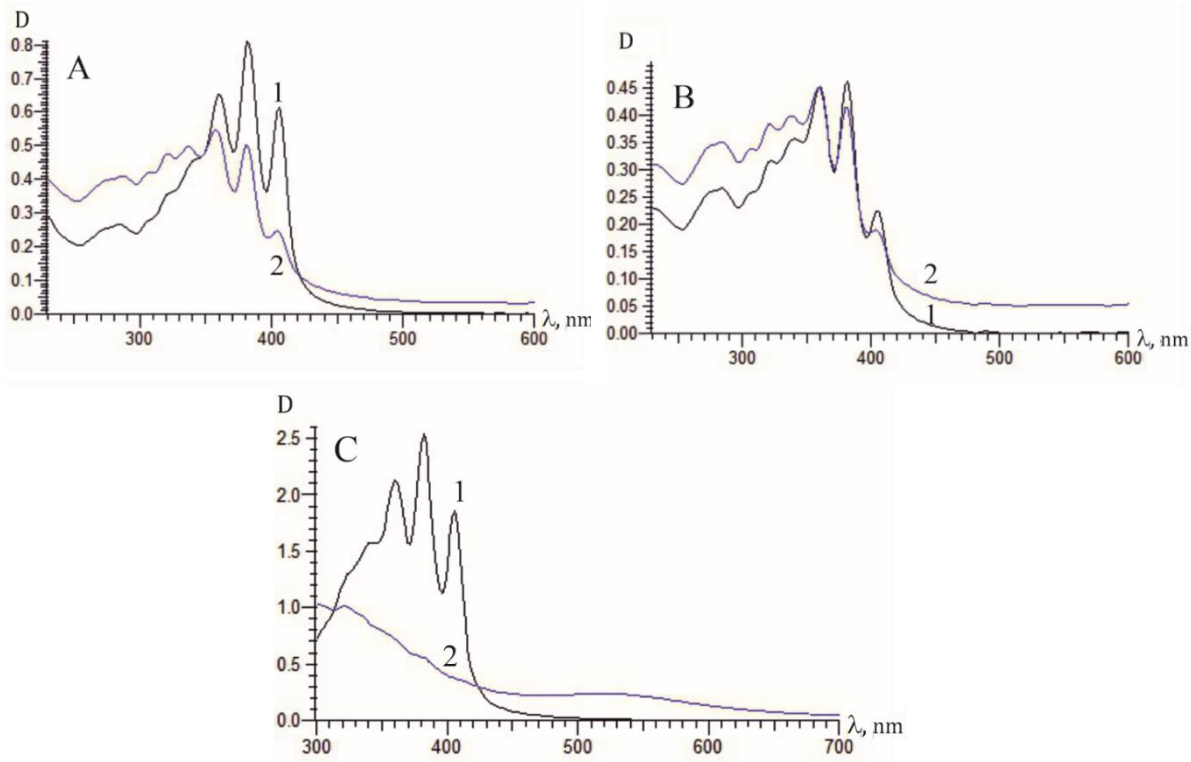

Figure 3. UV-Vis spectra. **(A)** AmB-Sub (1) and AmB-Sub Ox (2); **(B)** AmB-Med (1) and AmB-Med Ox (2); **(C)** AmB-Sub (1) and AmB-Sub/Au^0 (2).

For amphotericin composites with silver nanoparticles, the region $\lambda = 390–408$ nm overlaps with the absorption of silver nanoparticles; the possibility of amphotericin oxidation in this case was investigated by analyzing the corresponding fluorescence spectra. It has been shown in Refs. [28,29] that the fluorescence spectra of amphotericin were changed in the

presence of an oxidizing agent (Fe^{3+} or KMnO4) with an increase in the band at 471 nm (emission spectra, Ex 350 nm). Under our conditions, we did not notice an increase in the 471 nm band for the AmB/Ag^o samples (Figure 4), which suggests that amphotericin is not oxidized during the preparation of the conjugate AmB/Ag^o. In this case, the thermodynamic prerequisites for the reduction of silver cations in an alkaline medium should also be taken into account. These conditions are described in detail in our previous publication [25].

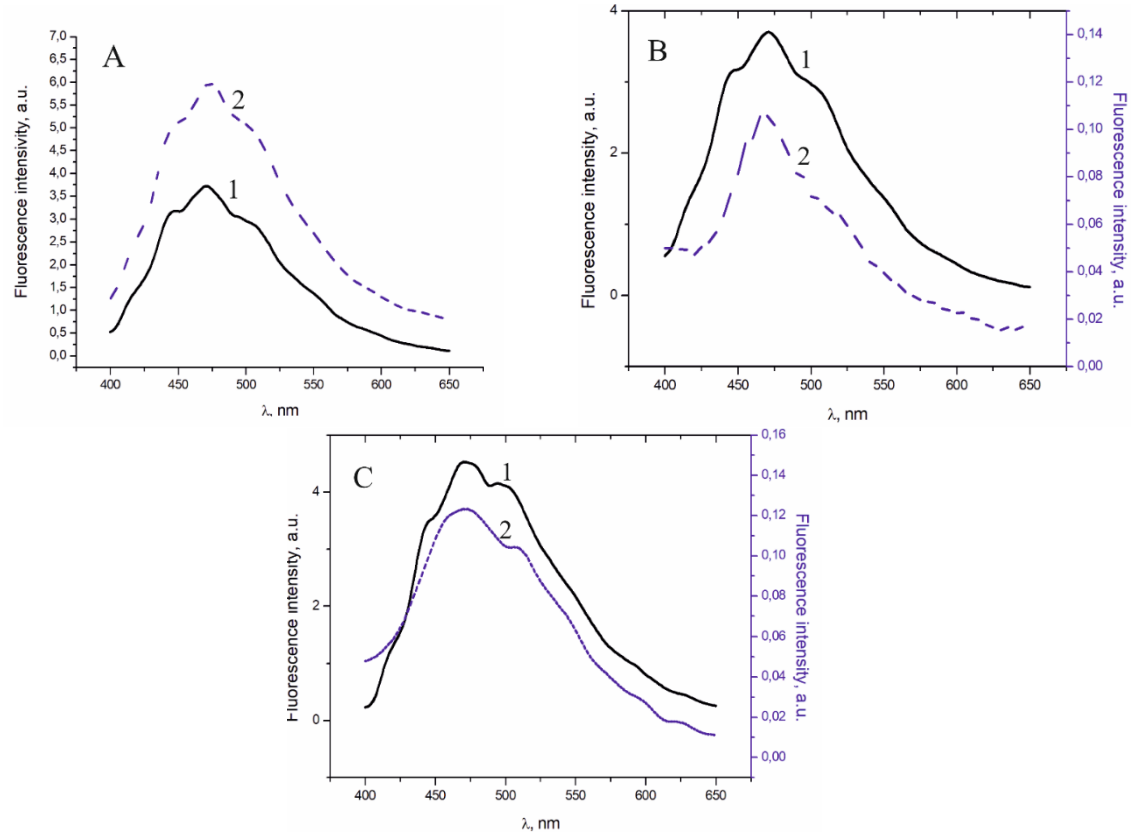

Figure 4. Fluorescence spectra. **(A)** AmB-Med (1) and AmB-Med Ox (2); **(B)** AmB-Med (1) and AmB-Med/Ag^0 (T) (2); **(C)** AmB-Sub (1) and AmB-Sub/Ag^0 (T) (2).

As an alternative procedure for preparing the amphotericin/silver nanoparticle composite, we tested microwave (MW) irradiation (method B). This strategy ensures rapid, uniform, and volumetric heating of the reaction medium and high reaction rates; the reaction system is heated by the high-frequency reciprocating motion of the internal molecular dipole, which absorbs microwave energy and converts it into thermal energy [30-32]. Under the influence of microwave radiation on water, solvated electrons are formed, which participate in the reduction of metal cations [33]: $Ag^+ + e^{aq-} \rightarrow Ag^0$. MW irradiation is environmentally friendly, requires less energy than conventional methods, and can shorten reaction time. This approach also does not involve handling potentially contaminated or cytotoxic reducing agents.

Figure 5 shows the formation of amphotericin/silver nanocomposites using the MW irradiation method: AmB-Sub/Ag^0(M) and AmB-Med/Ag^0(M).

As can be seen from Figure 5, the plasmon resonance peak of silver nanoparticles is centered at λ = 410-420 nm over time, both for the AmB-Sub/Ag^0 (Figure 5a) sample and for AmB-Med/Ag^0 (Figure 5b). In both cases, the reaction is almost complete after 2 minutes of observation. Therefore, this method (B) allows a reduction in reaction time by approximately 10 times compared to conventional heating of the reaction medium (A) at the same pH and temperature.

Method C involves introducing an external reducing agent - $NaBH_4$ for silver nanoparticle preparation. Figure 6 shows the formation of amphotericin/silver nanocomposites using $NaBH_4$.

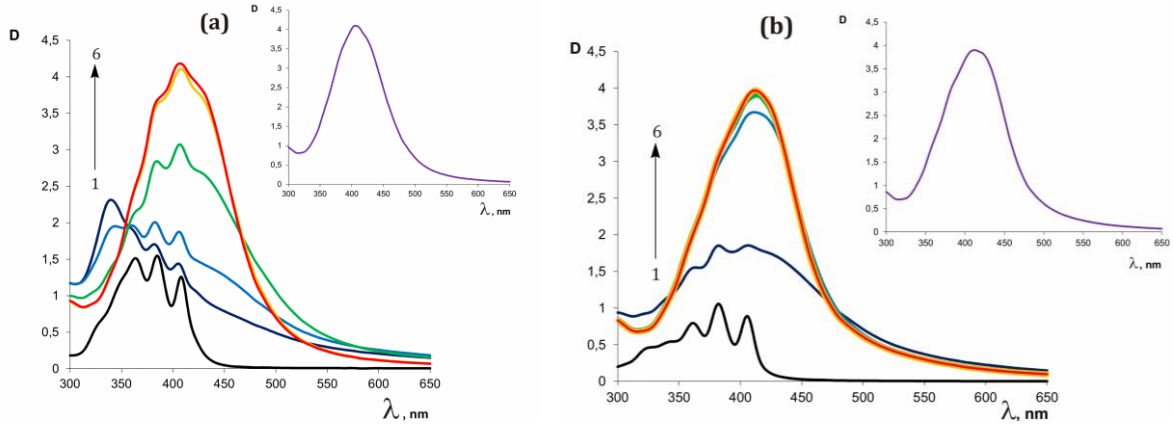

Figure 5. Kinetics of forming of composites: **(a)** AmB-Med/Ag^0(M); **(b)** AmB-Sub/Ag^0(M) under microwave irradiation. AmB concentration 0.05 mg/mL, the ratio AmB/Ag^+ 1:14 (mol). Spectra recording time: 0, 0.5, 1.0, 1.5, 2.0, 2.5 min. (from 1 to 6). The insets show spectra after 1 day of storage.

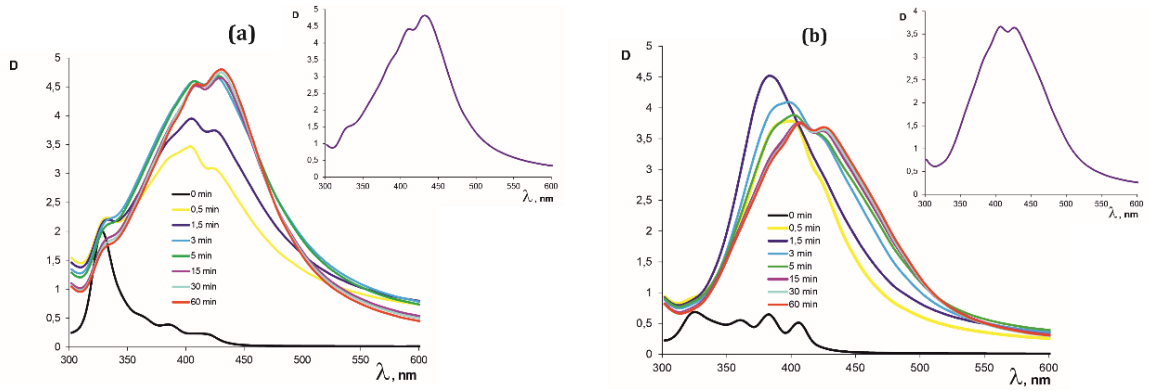

Figure 6. Composites formation: **(a)** AmB-Med/Ag^0(B); **(b)** AmB-Sub/Ag^0(B) after $NaBH_4$ reduction of silver cations. The ratio AmB/Ag^+/$NaBH_4$ (mol) was 1:14:28. The insets show spectra after 1-day storage.

Unlike the above methods A and B, when using a reducing agent ($NaBH_4$) for silver reduction, an increase in absorption at 380 nm was recorded at the first stage of synthesis. This is especially noticeable when using the amphotericin substance (Figure 6b). It was previously shown that long-lived "magic" silver clusters exhibit a peak at 380 nm in UV absorption experiments due to the excitation of a plasmon [34]. The calculated absorption band maxima for clusters Ag 5 to Ag 12 are located between 300 and 400 nm [35]. During the reaction, a peak corresponding to the nanoform of silver is formed within 30 min. The probability of oxidation of amphotericin during the production of AmB/Ag^0 composites using sodium borohydride is also very low. $NaBH_4$ is a very strong reducing agent - standard redox potential –1.24 V. It is also known that the deoxycholate present in the drug form of amphotericin is not oxidized by silver cations, as was shown in the production of silver nanoparticles with $NaBH_4$ [36].

In composites based on the amphotericin substance, the size of silver nanoparticles, regardless of the method of their formation, is in the range of 6-10 nm (Figures 7b-d), which approximately corresponds to the range of nanoparticle sizes in the case of polymer-stabilized nanosilver (Figure 7a). For the gold-containing AmB-Sub/Au^0(T) composite, gold nanoparticles were almost uniform and predominantly 6 nm in size (Figure 7e). As to the drug-based composites - AmB-Med/Ag^0 (Figures 7f-h), larger nanoparticles are found in systems. The size of visualized spheres is possibly due to the impact of the deoxycholate coat, which is

not separated visually. In this case, 70-80% of the particles fall within the range of more than 25 nm for methods with heating of the reaction mixture (Figures 7f,g) and approximately 30% when using a reducing agent (Figure 7h).

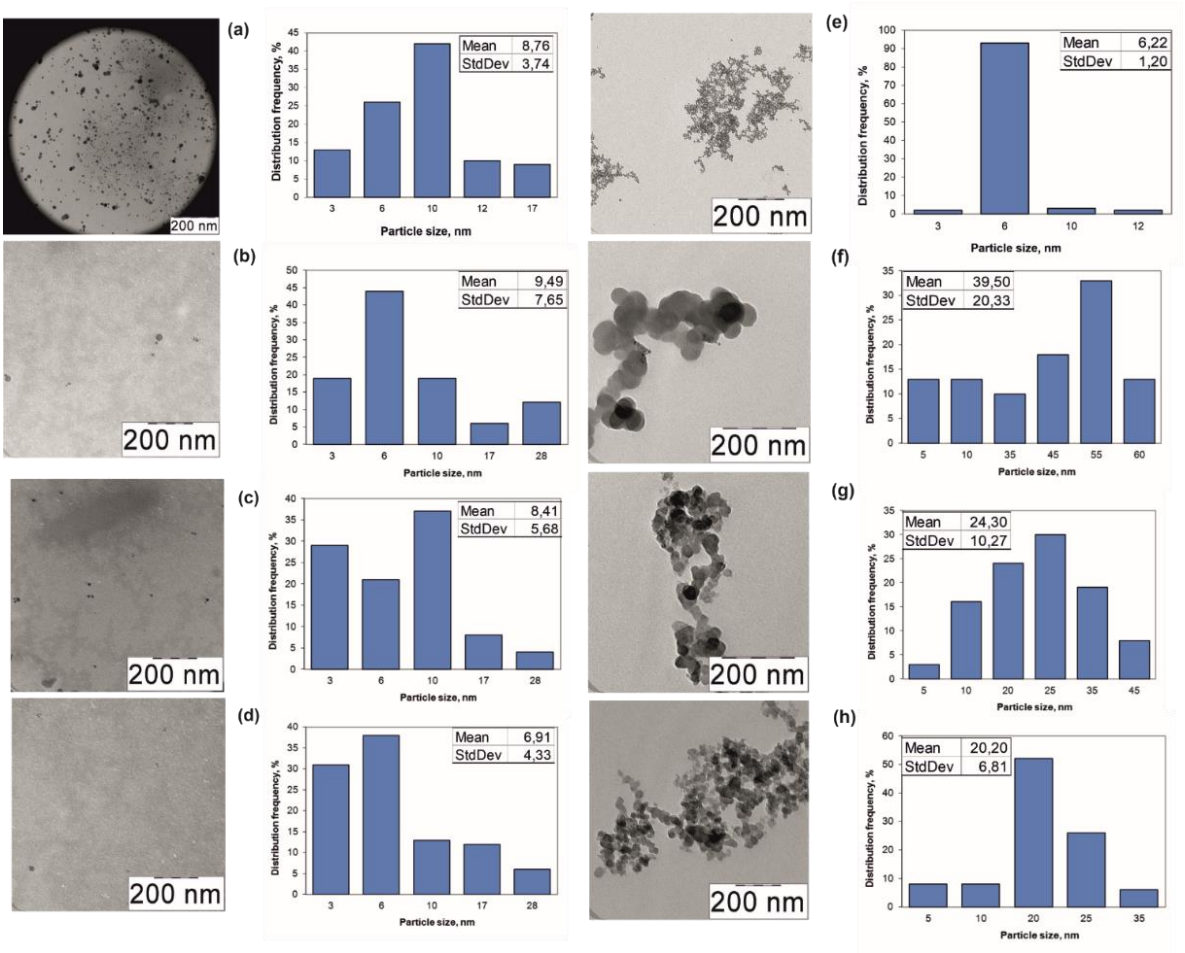

Figure 7. TEM images of samples: **(a)** EM/Ag^0; **(b)** AmB-Sub/Ag^0 (T); **(c)** AmB-Sub/Ag^0 (M); **(d)** AmB-Sub/Ag^0 (B); **(e)** AmB-Sub/Au^0 (T); **(f)** AmB-Med/Ag^0 (T); **(g)** AmB-Med/Ag^0 (M); **(h)** AmB-Med/Ag^0 (B).

Changes in particle size distribution in the course of AmB/Ag^0 compositions preparation were tested by the DLS method. As an example, Figure 8 shows the kinetics of the formation of the AmB-Sub/Ag^0 (T) composite.

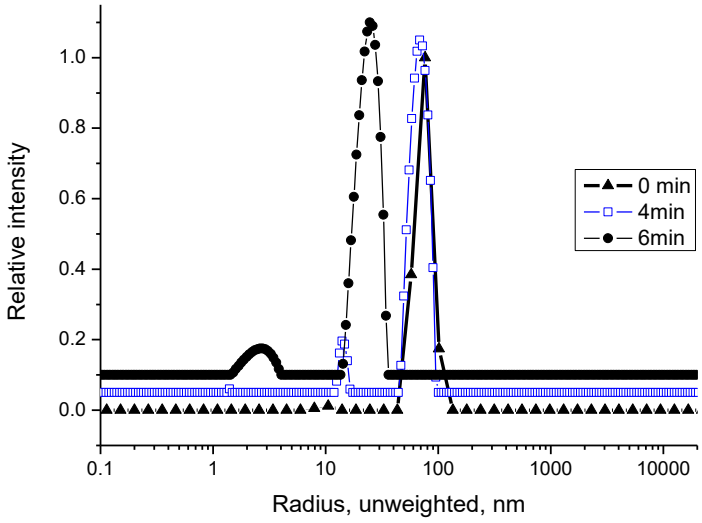

Figure 8. Changes in particle size distribution during the formation of AmB-Sub/Ag^0 (T) composite. Scattering angle – 90°.

The initial mixture contained relatively large nanoparticles (R_h =73 nm), formed by hydrophobic polyene substance AmB. As silver reduction occurred, smaller nanoparticles of the AmB/Ag0 complex appear in the mixture (a small peak with Rh = 14 nm after 4 min). A sharp transition in particle size distribution occurred between 4 and 6 min of heating: after 6 min, the size distribution demonstrated two peaks with hydrodynamic radii R_h = 2.5 and 24 nm. One should note that the light scattering intensity (I) is related to the mass fraction of particles (c) by the following relation: I = ~ c M, where M is the molar mass of the particle. Therefore, the particles, having an order-of-magnitude larger size and demonstrating a large scattering intensity, constitute a small mass fraction in the mixture. This distribution can be explained by the presence of individual metal nanoparticles coated with an AmB shell and micellar aggregates of the same NPs formed within the AmB aggregates. A similar phenomenon was observed when producing polymer-stabilized silver NPs [37], but in the presence of the polymer, such aggregates were typically larger ($R_h \approx 100$ nm). The presence of this type of aggregate does not lead to a change in the plasmon spectrum. Thus, the DLS results indicate that the process of complex AmB-Sub/Ag^o particles formation is nearing completion after 6 minutes, which is in compliance with the UV-Vis study (Figure 1b).

The size distributions of AmB/Ag^0 complexes prepared by various techniques are shown in Figure 9.

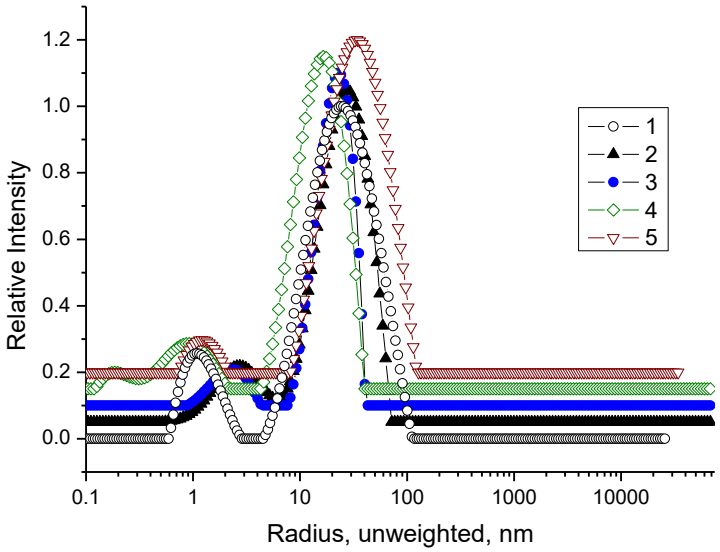

Figure 9. Size distributions of AmB/Ag^0 composites prepared by various methods: (1) AmB-Sub/Ag^0(B), (2) AmB-Sub/Ag^0(M), (3) AmB-Med/Ag^0(T), (4) AmB-Med/Ag^0(B), (5) AmB-Med/Ag^0(M). Scattering angle – 90°, concentration – 0.05 mg/mL.

Typical distributions with fast and slow modes, corresponding to R_h fast about 1 – 2 nm and R_h slow = 15 – 31 nm (Table 1), were obtained for all prepared nanocomposits.

Table 1. Hydrodynamic radii of AmB/Ag^0 composite particles prepared by various methods.

Sample	R_h^{fast}, nm (±RPW)	R_h^{slow}, nm (±RPW)
EM/Ag^{0*}	2	125
AmB-Sub/Ag^0(T)	2.5 (± 0.21)	24 (± 0.41)
AmB-Med/Ag^0(T)	2.2 (± 0.34)	21(± 0.36)
AmB-Sub/Ag^0(M)	2.1**	27**
AmB-Med/Ag^0(M)	1.7 (± 0.23)	31 (± 0.58)
AmB-Sub/Ag^0(B)	0.8 (± 0.38)	26 (± 0.64)
AmB-Med/Ag^0(B)	0.8 (± 0.66)	15 (± 0.45)

*Ref. [38].; ** The peaks are not completely separated.

DLS study shows that AmB-containing nanocomposites are rather similar to each other in their structure in solutions. The fraction of micellar aggregates (slow mode) is characterized by essentially smaller size compared with polymer-stabilized silver nanoparticles (EM/Ag0, Table 1).

ξ-potentials for the AmB-Sub/Ag^0 samples ranged from –13 to –22 mV, and more negative values from –25 to –29 mV were obtained for AmB-Med/Ag^0(M) (for all methods used). This difference reflects the impact of the negatively charged deoxycholate, which enhances the colloidal stability of the latter samples.

In this work, we investigated the antifungal activity of AmB/AgNPs composites in relation to one of the most common opportunistic fungal pathogens in humans – *C. albicans* (Table 2).

Table 2. The antifungal activities of the composites.

Sample	The content of components in the sample, % (weight)		MIC (mg/mL)[a]			FIC[b]		FICI[b]
	$Ag^0(Au^0)$	AmB	Sample[a]	$Ag^0(Au^0)$	AmB	Ag^0	AmB	
EM/Ag^0	43.0	-	76.9±15.0	33.1±6.4	-	-	-	
AmB-Sub	-	100	0.20±0.00	-	0.20	-	-	
AmB-Med	-	40	0.49±0.10	-	0.20±0.04	-	-	
AmB-Sub/Ag^0(T)	62.1	37.9	0.53±0.11	0.32±0.06	0.20±0.04	0.01	1.0	1.01
AmB-Sub/Ag^0(M)	62.1	37.9	0.53±0.11	0.32±0.06	0.20±0.04	0.01	1.0	1.01
AmB-Sub/Ag^0(B)	62.1	37.9	0.52±0.10	0.32±0.06	0.20±0.04	0.01	1.0	1.01
AmB-Sub/Au^0(T)	52.0	48.0	12.98±2.6	6.75±1.35	6.23±1.25	-	-	-
AmB-Med/Ag^0(T)	39.6	24.2	0.82±0.16	0.32±0.06	0.20±0.04	0.01	1.0	1.01
AmB-Med/Ag^0(B)	39.6	24.2	0.20±0.04	0.08±0.02	0.05±0.01	0.002	0.25	0.252

MIC – minimum inhibitory concentrations; FIC – Fractional Inhibitory Concentration; FICI – Fractional Inhibitory Concentration Index; [a] The MIC values were processed by mathematical statistics using Student's t – test; [b] FIC and FICI were calculated from the average MIC values.

In addition to MIC samples, MIC of bioactive components (AgNPs or AuNPs) present in the preparation are also given in terms of their content in the composite, which allows us to take into account their mutual influence on the activity of the drug. The degree of mutual influence of antimicrobial components (AgNP and AmB) in the prepared conjugates was assessed by calculating the Fractional Inhibitory Concentration (FIC) and the Fractional Inhibitory Concentration Index (FICI): FIC (Ag0) = MIC (Ag0 in combination with AmB)/MIC (Ag0 in control); FIC (AmB) = MIC (AmB in combination with Ag0)/MIC (AmB alone); FICI = FIC (Ag0) + FIC (AmB). From the data presented in Table 2, it follows that the MIC of amphotericin in the composites with silver nanoparticles (in terms of its content in the samples - FIC values) practically does not decrease for all samples. This indirectly indicates the immutability of the antibiotic structure. For the AmB-Sub/Au0(T), the MIC sample and FIC value of amphotericin are significantly higher than those for all composites containing silver nanoparticles. This may be due to both the low antifungal activity of gold nanoparticles and the conversion of amphotericin to a less active oxidized form during the reaction (Figure 3).

It can also be noted that the activity of silver nanoparticles in the complexes with amphotericin increased in comparison with their activity in the control composite, where silver nanoparticles were stabilized by a copolymer of maleic acid with ethylene (EM/Ag^o) [22]. With similar sizes of silver nanoparticles, this is apparently explained by differences in the structure and size of the stabilizing shell, for the low-molecular stabilizer amphotericin and the high-

molecular copolymer. The association of AmB with nanoparticles may have allowed for more efficient delivery of metal nanoparticles into fungal cellular structures.

For silver-containing samples, when considering the FICI values, which take into account the contribution of AmB and AgNPs to the activity of the drug, it is clear that all these values do not exceed 1.01. FICI values between 0.5 and 2.0 indicate an additive effect, as previously shown [39]. Antagonism of bioactive components was defined by FICI values >4.0, and additive interaction was defined by FICI values between >0.5 and 4.0 [40]. Synergistic interactions were defined when the FICI was equal to or less than 0.5, and this point of view was shared by all the mentioned researchers [39,40]. In light of the above-mentioned literature data, the obtained values of FICI = 1.01 can be interpreted as additive participation of active components in composites, and for the composite AmB-Med/Ag^o(B) - synergistic participation. In the latter case, the observed effect can apparently be explained by the smaller size of the composite particles (DLS method), which is important for the effective delivery of bioactive components into the fungal cellular structures. The molecular organization and particle size of the drug play key roles in its activity [41]. It has been shown that AmB/Ag^o can effectively cross the cell wall barrier of the fungus [42].

4. Conclusions

Three one-pot variants for preparing water-soluble composites of amphotericin and silver nanoparticles are proposed, in which the antibiotic serves as a stabilizer for metal nanoparticles formed in its presence. In the first approach, the reaction leading to metal nanoparticle formation occurred in an alkaline medium upon heating; in the second, electromagnetic radiation was used to influence the system; in the third, a reducing agent was introduced. Amphotericin B substance and amphotericin B medicine were used in this study. The formation of AgNPs for both amphotericin samples upon heating (70°C) and at a pH of 10 is almost complete within 20 minutes. Compared to the above-mentioned method, the approach based on microwave radiation at the same temperature and pH values made it possible to reduce the reaction time by about 10 times. When using $NaBH_4$ as a reducing agent for silver cations, amphotericin/silver nanoparticles complexes were formed in 30 minutes. For each of the antibiotic samples, when using all three options for nanoparticle synthesis, the physicochemical parameters of the obtained AmB/Ag^o complexes turned out to be similar.

When studying the antifungal activity of preparations against C. albicans, additive participation of bioactive components in all AmB/Ag^o composites was revealed, with the exception of the preparation based on medicine AmB (borohydride method), where synergistic participation of the system components was revealed. Synthesis of gold nanoparticles in the presence of amphotericin resulted in the formation of a corresponding complex with amphotericin activity lower than that of the original antibiotic, apparently due to oxidation of the latter.

The proposed approaches do not use organic solvents or complex equipment.

Author Contributions

Conceptualization, N.S.; methodology, N.S., O.V., N.A., and D.P.; validation, O.V. and D.P.; formal analysis, N.S. and I.B.; investigation, N.S., M.K., I.B., O.V., and N.A.; resources, D.P.; writing—original draft preparation, M.K., I.B., and D.P.; writing—review and editing, N.S.;

visualization, N.A.; project administration, N.S. All authors have read and agreed to the published version of the manuscript.

Institutional Review Board Statement

Not applicable.

Informed Consent Statement

Not applicable.

Data Availability Statement

Data can be available upon request.

Funding

This work was supported by the Ministry of Science and Higher Education of the Russian Federation (Contract No. 075-03-2026-024) and was performed using equipment at the Center for Collective Use of INEOS RAS.

Acknowledgments

The TEM study was conducted under the state assignment of Lomonosov Moscow State University.

Conflicts of Interest

The authors declare no competing interests.

References

1. Zielińska, J.; Wieczór, M.; Chodnicki, P.; Grela, E.; Luchowski, R.; Nierzwicki, Ł.; Bączek, T.; Gruszecki, W.I.; Czub, J. Self-assembly, stability and conductance of amphotericin B channels: bridging the gap between structure and function. *Nanoscale* **2021**, *13*, 3686-3697, https://doi.org/10.1039/d0nr07707k.
2. Umegawa, Y.; Yamamoto, T.; Dixit, M.; Funahashi, K.; Seo, S.; Nakagawa, Y.; Suzuki, T.; Matsuoka, S.; Tsuchikawa, H.; Hanashima, S.; Oishi, T.; Matsumori, N.; Shinoda, W.; Murata, M. Amphotericin B assembles into seven-molecule ion channels: An NMR and molecular dynamics study. *Sci. Adv.* **2022**, *8*, eabo2658, https://doi.org/10.1126/sciadv.abo2658.
3. Anderson, T.M.; Clay, M.C.; Cioffi, A.G.; Diaz, K.A.; Hisao, G.S.; Tuttle, M.D.; Nieuwkoop, A.J.; Comellas, G.; Maryum, N.; Wang, S.; Uno, B.E.; Wildeman, E.L.; Gonen, T.; Rienstra, C.M.; Burke, M.D. Amphotericin forms an extramembranous and fungicidal sterol sponge. *Nat. Chem. Biol.* **2014**, *10*, 400-406, https://doi.org/10.1038/nchembio.1496.
4. Kovacic, P.; Cooksy, A. Novel, unifying mechanism for amphotericin B and other polyenedrugs: electron affinity, radicals, electron transfer, autoxidation, toxicity, and antifungal action. *Med. Chem. Commun*. **2012**, *3*, 274–280, https://doi.org/10.1039/c2md00267a.
5. Boudier, A.; Mammari, N.; Lamouroux, E.; Duval, R.E. Inorganic Nanoparticles: Tools to Emphasize the Janus Face of Amphotericin B. *Antibiotics* **2023**, *12*, 1543, https://doi.org/10.3390/antibiotics12101543.
6. O'Shaughnessy, E.M.; Lyman, C.A.; Walsh, T.J. Amphotericin B: Polyene Resistance Mechanisms. In Antimicrobial Drug Resistance: Mechanisms of Drug Resistance, Mayers, D.L., Ed.; Humana Press: Totowa, NJ, **2009**; pp. 295-305, https://doi.org/10.1007/978-1-59745-180-2_25.
7. Sanglard, D.; Odds, F.C. Resistance of *Candida* species to antifungal agents: molecular mechanisms and clinical consequences. *Lancet Infect. Dis.* **2002**, *2*, 73–85, https://doi.org/10.1016/s1473-3099(02)00181-0.

8. Jenkinson, H.F.; Douglas, L.J. Interactions between Candida species and bacteria in mixed infections. In Polymicrobial Diseases; Brogden, K.A., Guthmiller, J.M., Eds.; ASM Press: Washington, DC, USA, **2002**; pp. 357–373, https://doi.org/10.1128/9781555817947.ch18.
9. Mubeen, B.; Ansar, A.N.; Rasool, R.; Ullah, I.; Imam, S.S.; Alshehri, S.; Ghoneim, M.M.; Alzarea, S.I.; Nadeem, M.S.; Kazmi, I. Nanotechnology as a Novel Approach in Combating Microbes Providing an Alternative to Antibiotics. *Antibiotics* **2021**, *10*, 1473, https://doi.org/10.3390/antibiotics10121473.
10. Samoilova, N.; Krayukhina, M.; Popov, D.; Anuchina, N. Specific effects and features of a combination of amine-containing antibacterial agents and silver nanoparticles stabilized by dicarboxylic acid copolymers. *Monatsh. Chem.* **2019**, *150*, 2071-2080, https://doi.org/10.1007/s00706-019-02523-2.
11. Kumar, P.; Shivam, P.; Mandal, S.; Prasanna, P.; Kumar, S.; Prasad, S.R.; Kumar, A.; Das, P.; Ali, V.; Singh, S.K. Synthesis, characterization, and mechanistic studies of a gold nanoparticle–amphotericin B covalent conjugate with enhanced antileishmanial efficacy and reduced cytotoxicity. *Int. J. Nanomedicine* **2019**, *14*, 6073-6101, https://doi.org/10.2147/IJN.S196421.
12. Gouyau, J.; Duval, R.E.; Boudier, A.; Lamouroux, E. Investigation of Nanoparticle Metallic Core Antibacterial Activity: Gold and Silver Nanoparticles against *Escherichia coli* and *Staphylococcus aureus*. *Int. J. Mol. Sci.* **2021**, *22*, 1905, https://doi.org/10.3390/ijms22041905.
13. Singh, P.; Mijakovic, I. Antibacterial Effect of Silver Nanoparticles Is Stronger If the Production Host and the Targeted Pathogen Are Closely Related. *Biomedicines* **2022**, *10*, 628, https://doi.org/10.3390/biomedicines10030628.
14. Casals, E.; Gusta, M.F.; Bastus, N.; Rello, J.; Puntes, V. Silver Nanoparticles and Antibiotics: A Promising Synergistic Approach to Multidrug-Resistant Infections. *Microorganisms* **2025**, *13*, 952, https://doi.org/10.3390/microorganisms13040952.
15. Mijnendonckx, K.; Leys, N.; Mahillon, J.; Silver, S.; Van Houdt, R. Antimicrobial silver: uses, toxicity and potential for resistance. *BioMetals* **2013**, *26*, 609-621, https://doi.org/10.1007/s10534-013-9645-z.
16. Rajendran, K.; Anwar, A.; Khan, N.A.; Siddiqui, R. Brain-Eating Amoebae: Silver Nanoparticle Conjugation Enhanced Efficacy of Anti-Amoebic Drugs against *Naegleria fowleri*. *ACS Chem. Neurosci.* **2017**, *8*, 2626-2630, https://doi.org/10.1021/acschemneuro.7b00430.
17. Victoria, L.; Roxana, V.A.; Adrian, M.; Dante, M.B. Silver Nanoparticles with High Loading Capacity of Amphotericin B: Characterization, Bactericidal and Antifungal Effects. *Curr. Drug Deliv.* **2018**, *15*, 850-859, https://doi.org/10.2174/1567201814666170918162337.
18. Ahmad, A.; Wei, Y.; Syed, F.; Tahir, K.; Taj, R.; Khan, A.U.; Hameed, M.U.; Yuan, Q. Amphotericin B-Conjugated Biogenic Silver Nanoparticles as an Innovative Strategy for Fungal Infections. *Microb. Pathog.* **2016**, *99*, 271–281, https://doi.org/10.1016/j.micpath.2016.08.031.
19. Nadhe, S.B.; Singh, R.; Wadhwani, S.A.; Chopade, B.A. Acinetobacter sp. mediated synthesis of AgNPs, its optimization, characterization and synergistic antifungal activity against *C. albicans*. *J. Appl. Microbiol.* **2019**, *127*, 445-458, https://doi.org/10.1111/jam.14305.
20. Ayaz, A.; Ruqaiyyah, S.; Muhammad, S.; Naveed, K. Gold Nanoparticles Conjugation Enhances Antiacanthamoebic Properties of Nystatin, Fluconazole and Amphotericin B. *J. Microbiol. Biotechnol.* **2019**, *29*, 171-177, https://doi.org/10.4014/jmb.1805.05028.
21. Tutaj, K.; Szlazak, R.; Szalapata, K.; Starzyk, J.; Luchowski, R.; Grudzinski, W.; Osinska-Jaroszuk, M.; Jarosz-Wilkolazka, A.; Szuster-Ciesielska, A.; Gruszecki, W.I. Amphotericin B-silver hybrid nanoparticles: synthesis, properties and antifungal activity. *Nanomed.: Nanotechnol. Biol. Med.* **2016**, *12*, 1095-1103, https://doi.org/10.1016/j.nano.2015.12.378.
22. Samoilova, N.; Kurskaya, E.; Krayukhina, M.; Askadsky, A.; Yamskov, I. Copolymers of Maleic Acid and Their Amphiphilic Derivatives as Stabilizers of Silver Nanoparticles. *Phys. Chem. B* **2009**, *113*, 3395-3403, https://doi.org/10.1021/jp806683m.
23. Clinical and Laboratory Standards Institute. Methods for Dilution Antimicrobial Susceptibility Tests for Bacteria That Grow Aerobically; Approved Standard—Ninth Edition. CLSI document M07-A9. Clinical and Laboratory Standards Institute, Wayne, Pennsylvania, USA, **2012**.
24. Samoilova, N.; Krayukhina, M.; Naumkin, A.; Anuchina, N.; Popov, D. Silver nanoparticles doped with silver cations and stabilized with maleic acid copolymers: specific structure and antimicrobial properties. *New J. Chem.* **2021**, *45*, 14513-14521, https://doi.org/10.1039/d1nj02478g.
25. Samoilova, N.A.; Krayukhina, M.A.; Korlyukov, A.A.; Klemenkova, Z.S.; Naumkin, A.V.; Mezhuev, Y.O. One-Pot Synthesis of Colloidal Hybrid Au (Ag)/ZnO Nanostructures with the Participation of Maleic Acid Copolymers. *Polymers* **2023**, *15*, 1670, https://doi.org/10.3390/polym15071670.

26. Gallardo, O.A.D.; Moiraghi, R.; Macchione, M.A.; Godoy, J.A.; Pérez, M.A.; Coronado, E.A.; Macagno, V.A. Silver oxide particles/silver nanoparticles interconversion: susceptibility of forward/backward reactions to the chemical environment at room temperature. *RSC Adv.* **2012**, *2*, 2923–2929, https://doi.org/10.1039/c2ra01044e.
27. Klimek, K.; Strubińska, J.; Czernel, G.; Ginalska, G.; Gagoś, M. *In vitro* evaluation of antifungal and cytotoxic activities as also the therapeutic safety of the oxidized form of amphotericin B. *Chem. -Biol. Interact.* **2016**, *256*, 47-54, https://doi.org/10.1016/j.cbi.2016.06.022.
28. Czernel, G.; Typek, R.; Klimek, K.; Czuryło, A.; Dawidowicz, A.L.; Gagoś, M. Catalytic effect of free iron ions and heme-iron on chromophore oxidation of a polyene antibiotic amphotericin B. *J. Mol. Struct.* **2016**, *1111*, 69-75, http://dx.doi.org/10.1016/j.molstruc.2016.01.052.
29. Gagoś, M.; Czernel, G. Oxidized forms of polyene antibiotic amphotericin B. *Chem. Phys. Lett.* **2014**, *598*, 5–9, http://dx.doi.org/10.1016/j.cplett.2014.02.052.
30. Singh, C.; Khanna, V.; Singh, S. Sustainability of microwave heating in materials processing technologies. *Mater. Today: Proc.* **2023**, *73*, 241–248, https://doi.org/10.1016/j.matpr.2022.07.216.
31. Patel, K.; Kapoor, S.; Dave, D.P.; Mukherjee, T. Synthesis of nanosized silver colloids by microwave dielectric heating. *J. Chem. Sci.* **2005**, *117*, 53–60, https://doi.org/10.1007/BF02704361.
32. Afolayan, J.S.; Varney, A.M.; Thomas, J.C.; McLean, S.; Perry, C.C. A rapid microwave approach for 'one-pot' synthesis of antibiotic conjugated silver nanoparticles with antimicrobial activity against multi-drug resistant bacterial pathogens. *Colloids Surf. B: Biointerfaces* **2025**, *245*, 114280, https://doi.org/10.1016/j.colsurfb.2024.114280.
33. Vaks, V.L.; Domrachev, G.A.; Rodygin, Y.L.; Selivanovskii, D.A.; Spivak, E.I. Dissociation of water by microwave radiation. *Radiophys. Quantum Electron.* **1994**, *37*, 85-88, https://doi.org/10.1007/BF01039308.
34. Ershov, B.G.; Janata, E.; Henglein, A. ChemInform Abstract: Growth of Silver Particles in Aqueous Solution: Long-Lived "Magic" Clusters and Ionic Strength Effects. *J. Phys. Chem.* **1993**, *97*, 339–343, https://doi.org/10.1002/chin.199316042.
35. Farshad, M.; Perera, D.C.; Rasaiah, J.C. Theoretical study of the stability, structure, and optical spectra of small silver clusters and their formation using density functional theory. *Phys. Chem. Chem. Phys.* **2021**, *23*, 25507-25517, https://doi.org/10.1039/d1cp04070g.
36. Wang, J.; Fei, K.-X.; Yang, X.; Zhang, S.-S.; Peng, Y.-X. Synthesis and Plasmonic Chiroptical Studies of Sodium Deoxycholate Modified Silver Nanoparticles. *Materials* **2018**, *11*, 1291, https://doi.org/10.3390/ma11081291.
37. Samoilova, N.A.; Blagodatskikh, I.V.; Kurskaya, E.A.; Krayukhina, M.A.; Vyshivannaya, O.V.; Abramchuk, S.S.; Askadskii, A.A.; Yamskov, I.A. Stabilization of silver nanoparticles with copolymers of maleic acid. *Colloid J.* **2013**, *75*, 409-420, https://doi.org/10.1134/S1061933X1304008X.
38. Samoilova, N.A.; Krayukhina, M.A.; Klimova, T.P.; Babushkina, T.A.; Vyshivannaya, O.V.; Blagodatskikh, I.V.; Yamskov, I.A. Oxidation of glucose to gluconic acid using a colloidal catalyst containing gold nanoparticles and glucose oxidase. *Russ. Chem. Bull.* **2014**, *63*, 1009-1016, https://doi.org/10.1007/s11172-014-0541-7.
39. Ruden, S.; Hilpert, K.; Berditsch, M.; Wadhwani, P.; Ulrich Anne, S. Synergistic Interaction between Silver Nanoparticles and Membrane-Permeabilizing Antimicrobial Peptides. *Antimicrob. Agents Chemother.* **2009**, *53*, 3538-3540, https://doi.org/10.1128/AAC.01106-08.
40. Gupta, A.; Saleh, N.M.; Das, R.; Landis, R.F.; Bigdeli, A.; Motamedchaboki, K.; Rosa Campos, A.; Pomeroy, K.; Mahmoudi, M.; Rotello, V.M. Synergistic antimicrobial therapy using nanoparticles and antibiotics for the treatment of multidrug-resistant bacterial infection. *Nano Futures* **2017**, *1*, 015004, https://doi.org/10.1088/2399-1984/aa69fb.
41. Starzyk, J.; Gruszecki, M.; Tutaj, K.; Luchowski, R.; Szlazak, R.; Wasko, P.; Grudzinski, W.; Czub, J.; Gruszecki, W.I. Self-Association of Amphotericin B: Spontaneous Formation of Molecular Structures Responsible for the Toxic Side Effects of the Antibiotic. *J. Phys. Chem. B* **2014**, *118*, 13821-13832, https://doi.org/10.1021/jp510245n.
42. Janik, S.; Grela, E.; Stączek, S.; Zdybicka-Barabas, A.; Luchowski, R.; Gruszecki, W.I.; Grudzinski, W. Amphotericin B-Silver Hybrid Nanoparticles Help to Unveil the Mechanism of Biological Activity of the Antibiotic: Disintegration of Cell Membranes. *Molecules* **2023**, *28*, 4687, https://doi.org/10.3390/molecules28124687.

Publisher's Note & Disclaimer